# Stress in evaporated films used in GaAs processing

W. A. Strifler
*Watkins Johnson Company, 3333 Hillview Avenue, Palo Alto, California 94304 and Department of Electrical Engineering, Stanford University, Stanford, California 94305*

C.W. Bates, Jr.
*Department of Materials Science and Department of Electrical Engineering, Stanford University, Stanford, California 94305*

(Received 28 September 1990; accepted 20 November 1990)

A simple and practical method is described for determining the residual stress in vapor deposited thin films that are less than 1000 Å in thickness. The method relies on the evaporation of thin films onto prefabricated micro-cantilever beams of $SiO_2$. The vertical deflection at the end of the beam is measured using an optical microscope to determine the average film stress with a resolution of 25 MPa. Calculations show that the vapor deposition of metal films onto these beams does not induce significant heating, so the thermal component of residual film stress is minimal. The micro-cantilever technique is used to measure the film stress in 500 Å films of Al, Ti, Pt, Au, Ni, and Ge. These measured values are compared to similar measurements reported in the literature.

## I. INTRODUCTION

In silicon IC processing, aluminum serves as the work-horse metal film and can adequately provide for ohmic contacts, via plugs, contacts, and bond pads. GaAs processing is somewhat different from its silicon counterpart in that a more diverse selection of metal films is required to form the necessary circuit elements in a GaAs IC. Ohmic contacts to N-type GaAs usually involve the alloying of composite metal films containing Au, Ge, and Ni. Since the ohmic contact is gold based, it is natural to use a gold-based interconnect metal. A typical interconnect formulation would include Ti, Pt, and Au. The Ti serves as an adhesion layer while the Pt serves as a diffusion barrier to prevent reactions between the underlying GaAs and the Au top layer. Finally, Al is often used to make the critical Schottky barriers in the MESFET and diode devices.

For the case of GaAs processing, the mechanical stress in evaporated films is important for two fundamental reasons. Since GaAs is a piezoelectric material, the stress in attached metal films can induce strain and resulting polarization charge in the GaAs material. As an example of the magnitudes involved, a 2000 Å metal film with a stress of 500 MPa can induce a charge density of $10^{16}$ e/cm$^3$ in the underlying GaAs if the film is patterned with narrow openings.[1] Since the doping densities in typical GaAs devices are on the order of $10^{17}$/cm$^3$, the piezoelectric charge density can induce noticeable changes in device performance.

A second important aspect of metal film stress stems from the problem of patterning gold-based films on GaAs. GaAs is chemically reactive compared to Au, so it is difficult to selectively etch Au against GaAs. Thus it is necessary to pattern most metal films on GaAs using a lift-off technique whereby a photoresist pattern is created first, and the metal film is evaporated through the openings in the resist. This is followed by a solvent spray during which the underlying resist is dissolved and the unwanted metal is lifted off and washed away. The success of this lift-off technique depends directly on the stresses present in the metal film. If the tensile stress in the film is too great, then the forces acting on the edges of the photoresist can cause resist peeling during deposition, a catastrophic failure. More subtle problems can be related to stress gradients within a composite film. If the stress distribution within a film is such that it causes the film to curl away from the GaAs surface during solvent spray, then the lift-off proceeds quickly because the curling film continually exposes the underlying photoresist to fresh solvent. If the film curls toward the substrate during solvent spray, then the film tends to trap the photoresist and impede resist dissolution, so the lift-off process would proceed slowly in this case.

This paper reports the results of measurements to determine the average stress present in very thin (500 Å) evaporated films of Al, Ti, Pt, Au, Ni, and Ge used in GaAs processing. The small resulting edge force for these thin films necessitates the use of a micro-cantilever-beam technique for determining film stress.[2] Since these beams are fabricated before metal deposition, one critical question that arises is the degree of beam heating during deposition. This is important because the beam deflection is measured at room temperature, so the magnitude of heating must be known to determine the thermal component of film stress and in-

 

terpret the results. Part of this paper is devoted to answering this temperature question. Finally, the stress measurements from this work are compared to similar measurements reported in the literature.

## II. EXPERIMENTAL

### A. The micro-cantilever-beam technique

The technique for measuring film stress in this study is a variant of the micro-cantilever-beam technique described by Hong *et al.*[2] The structure of the cantilever beams is shown in Fig. 1. The beams are patterned in 1 $\mu$m of CVD $SiO_2$ on a semi-insulating GaAs substrate. The $SiO_2$ beams are etched in a $CF_4$-containing plasma, and the GaAs is etched out from under the beams to a depth of approximately 15 $\mu$m using a $H_2SO_4:H_2O_2:H_2O$ etchant. The beam width is 5 $\mu$m, and the beam length is 120 $\mu$m. The GaAs substrate choice is somewhat arbitrary for beam preparation, but it does offer some distinct advantages over a Si substrate. Many simple etches are available to etch GaAs quickly and provide near perfect selectivity to $SiO_2$. The choices for etching Si through a $SiO_2$ mask with high selectivity are very limited and more difficult to prepare.[2] Cleaving a wafer into many small samples is also simpler for a GaAs substrate due to the strong cleavage planes along the (110) surfaces.

When a film is deposited onto the cantilever beams, the stress in the film causes a vertical deflection in the beam, $\delta$. Since the film thickness used in this study is 20 times smaller than the beam thickness, the thin film approximation is still valid. In the limit of $\delta \ll L$, the total film stress is given by

$$\sigma_{tot} = Mt^2\delta/(3L^2h) \quad (1)$$

where $M$ is the biaxial modulus of the $SiO_2$ estimated[3] at 98 GPa, $t$ is the thickness of the $SiO_2$, $\delta$ is the vertical deflection at the end of the beam, $L$ is the length of the beam, and $h$ is the thickness of the evaporated film. The vertical deflection is determined using an optical microscope by comparing the focus depth at the end of the beam to the focus depth of the surrounding $SiO_2$. The minimum resolvable $\delta$ is approximately 1 $\mu$m for this technique which, using Eq. (1), puts the minimum resolvable film stress at 50 MPa for a 500 Å film. The wafer curvature method would yield a minimum resolvable film stress of 1 GPa for the same film thickness assuming a 50 mm silicon substrate of 0.5 mm thickness with approximately 3 $\mu$m of center-to-edge deflection required to discern stress warpage over the background texture of the wafer. This simple comparison clearly demonstrates the advantage of the micro-cantilever technique for measuring stress in very thin films.

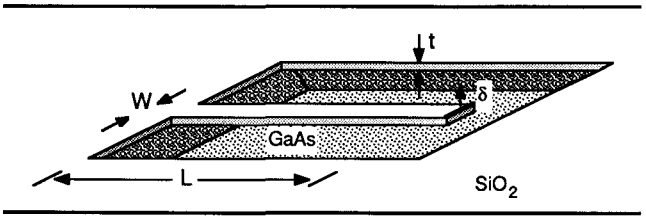


FIG. 1. Schematic diagram of a micro-cantilever beam.

### B. Deposition heating calculations

It is important to determine the rise in temperature that occurs along the beam during film deposition, so that one can distinguish between growth and thermal components in the total film stress. This temperature rise has the potential of being very large because of the large heat of condensation of the metal vapor and the low thermal mass of the thin $SiO_2$ beams. Table I lists the thermodynamic data[4] needed for this calculation. The cohesive energy is found by adding the heat of vaporization, the heat of solidification, and the specific heat needed to cool the liquid and solid phases down to room temperature. This calculation is very insensitive to the final temperature since the heat of vaporization comprises most of the cohesive energy. The cohesive energy along with the deposition rate determines the incident power onto the cantilever beam during deposition.

The next piece of information needed is the thermal mass of the $SiO_2$ beam. This is estimated at 0.17 mJ/(K cm$^2$) for a 1 $\mu$m thick layer.[5] If the beam were thermally isolated from its environment (not unreasonable since it is in a vacuum), then the rise in temperature from the deposition would be given by

$$\Delta T = (P_{inc})(t_{dep})/(m_{th}) \quad (2)$$

where $m_{th}$ is the thermal mass of the $SiO_2$, $P_{inc}$ is the incident power, and $t_{dep}$ is the total deposition time. This formula predicts a temperature rise of several hundred degrees Celsius for a 500 Å thick film. The calculation is incorrect, however, because it ignores the radiative heat transfer from the beam to its surroundings.

A more accurate model for the rise in temperature must include a radiative heat transfer term as in the

TABLE I. Data for calculating incident power onto a sample during film deposition.

| Element | Density (mol/cm$^3$) | Cohesive energy (Kcal/mol) | Standard dep. rate (Å/s) | Incident power (mW/cm$^2$) |
|---|---|---|---|---|
| Al | 0.100 | 84 | 20 | 7.0 |
| Ti | 0.094 | 124 | 5 | 2.5 |
| Pt | 0.110 | 149 | 10 | 6.9 |
| Au | 0.098 | 92 | 10 | 3.8 |
| Ni | 0.151 | 111 | 5 | 3.5 |
| Ge | 0.073 | 92 | 5 | 1.4 |

following differential equation:

$$(m_{th})dT/dt = P_{inc} - \epsilon\sigma(T^4 - T_0^4), \qquad T(0) = T_0 \tag{3}$$

where $\sigma$ is Stefan's constant, $\epsilon$ is the total hemispherical emittance of the beam surface, and $T_0$ is the temperature of the surroundings (blackbody assumed). Equation (3) makes the tacit assumption that the beam is uniform in temperature during the deposition. This is reasonable since the thermal time constant for the structure is tens of milliseconds while the deposition typically lasts for tens of seconds. It is also assumed that $\epsilon$ is constant with temperature, a good approximation over the limited range of temperatures reported in this work.

Equation (3) is simulated in Fig. 2 for various choices of emittance. The $\epsilon = 0$ case reduces to Eq. (2) and indicates a large rise in temperature. A smooth, bare surface of metal typically gives an emittance[6] of 0.01–0.03, which would yield a rise of temperature of a few hundred degrees.

Fortunately, the backside of the beam is better able to couple energy into the radiation field than the front side. The backside of the beam forms a $SiO_2$-coated metal surface which behaves differently from the bare metal front surface for two important reasons. First, the 1 $\mu$m film acts as a quarter-wave plate in the 7 $\mu$m infrared region of light, and this provides a better radiation impedance match between the vacuum and the metal surface. The 7 $\mu$m wavelength is essential because the blackbody spectrum at 400 K contains most of its energy near the 7 $\mu$m wavelength. The second important reason is that the $SiO_2$ has strong vibrational absorption bands in the 8–10 $\mu$m region which help it couple energy into the radiation field at precisely the range of wavelengths needed to give off heat at 300–400 K. These two factors together give an effective emittance[7] of 0.18, and this results in a total temperature rise of 50 °C (see Fig. 2), which is not a function of the $SiO_2$ thermal mass.

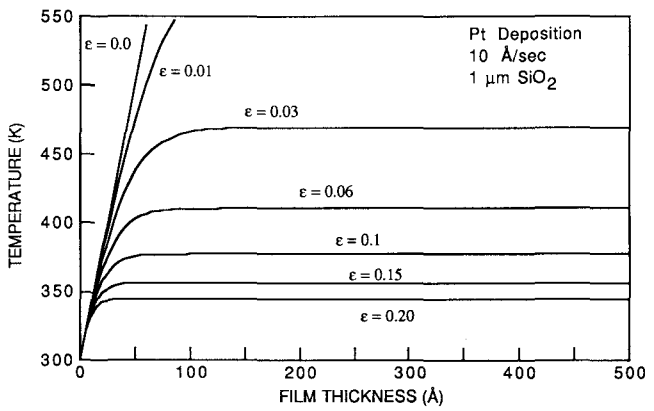


FIG. 2. Final cantilever-beam temperature as a function of deposited film thickness for various choices of total emittance.

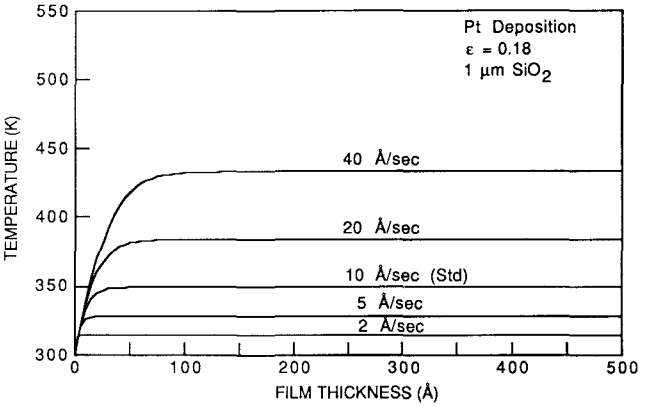


FIG. 3. Final cantilever-beam temperature as a function of film thickness for various deposition rates.

Figure 3 shows the same simulation for various deposition rates while holding the emittance of the structure constant. As expected, a larger deposition rate increases the equilibrium temperature, but the temperature is still constant over most of the deposition. Figure 4 shows the temperature profiles for the six metals deposited at their standard rates.

### C. Thermal stress calculation

During the film deposition, the film and the beam reach an equilibrium temperature, as determined in Fig. 4. After the deposition, the film/beam composite cools to room temperature, and the stress-induced deflection is measured. The process of cooling creates a thermal stress component due to the dissimilar expansion coefficients of the film and the $SiO_2$. The total measured stress is actually the sum of a growth stress from deposition and a thermal stress from cooling. In this section, the $\sigma_{thermal}$ component is calculated.

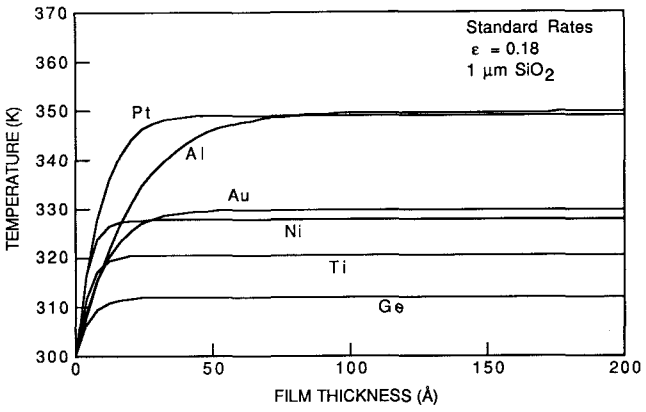


FIG. 4. Final cantilever-beam temperature as a function of film thickness for various elements deposited at the standard rates given in Table I.

TABLE II. Data for calculating the thermal component of film stress against $SiO_2$ due to a rise in temperature during deposition as predicted in Fig. 4. ($\sigma > 0$ = tension)

| Element | Average Young's modulus (GPa) | Average biaxial modulus (GPa) | Thermal expansion coefficient $\times 10^{-6}$/K | Induced $\sigma_{thermal}$ (MPa) |
|---|---|---|---|---|
| Al | 71 | 95 | 21.0 | 100 |
| Ti | 96 | 128 | 9.2 | 20 |
| Pt | 170 | 226 | 9.5 | 100 |
| Au | 77 | 103 | 14.0 | 40 |
| Ni | 196 | 260 | 13.2 | 90 |
| Ge | 137 | 182 | 5.8 | 10 |
| $SiO_2$ | *83* | *98* | *0.5* | *0* |

Table II shows the data for this calculation. A Young's modulus[8] averaged over all crystal directions is assumed and a Poisson's ratio of 0.25 is used to calculate the biaxial modulus of the evaporated films. The thermal expansion coefficients are also obtained,[8] and the temperature change is taken from Fig. 4. Since the films are all more expansive than the $SiO_2$ beam, the induced thermal stress is tensile, as shown in the last column. The magnitude of these stresses lies close to the minimum resolvable film stress for this particular measurement, so the $\sigma_{thermal}$ correction is not expected to be significant.

## III. RESULTS

500 Å films of Al, Ti, Pt, Au, Ni, and Ge are deposited onto the cantilever beams using a CHA electron beam evaporation system. The deposition rates are the same as shown in Table I. The vertical deflection of the cantilever ends is measured using an optical microscope, and Eq. (1) is used to calculate the film stress. Strictly speaking, Eq. (1) is accurate only for $\delta \ll L$, but the expression is still approximately true if

$$\cos(\theta) \approx 1 - \theta^2/2 \tag{4}$$

where $\theta = L/R$, and $R$ is the radius of curvature of the deflected beam. This approximation indicates that Eq. (1) gives $\sigma$ accurate to within 5% provided that $\delta$ is less than 30% of $L$. A vertical deflection of 0.30 $L$ corresponds to film stress of 2.0 GPa, so Eq. (1) is valid for all practical purposes.

Table III displays the results of these measurements. $\sigma_{total}$ is the total measured film stress as determined from $\delta$ and Eq. (1). $\sigma_{growth}$ is given by

$$\sigma_{growth} = \sigma_{total} - \sigma_{thermal} \tag{5}$$

where $\sigma_{thermal}$ is given in Table II.

## IV. DISCUSSION

The cantilever beam deflections were measured across several samples and found to be uniform within $\pm 0.5$ $\mu$m, so the precision uncertainty of $\sigma_{total}$ is approximately $\pm 25$ MPa. The accuracy of the measure-

TABLE III. Measured and reported values of total film stress. Growth stress is calculated by subtracting the thermal stress from Table II. ($\sigma > 0$ = tension)

| Element | Rate (Å/s) | $\sigma_{total}$ (MPa) | $\sigma_{growth}$ (MPa) | Substrate | Reference |
|---|---|---|---|---|---|
| Al | 20 | 80 | −20 | $SiO_2$ | This work |
| Ti | 5 | 830 | 810 | $SiO_2$ | This work |
| Pt | 10 | 1270 | 1170 | $SiO_2$ | This work |
| Au | 10 | 80 | 40 | $SiO_2$ | This work |
| Ni | 5 | 910 | 820 | $SiO_2$ | This work |
| Ge | 5 | 140 | 130 | $SiO_2$ | This work |
| Al | ? | 100 | | Quartz | Ref. 9 |
| Al | 60 | 20 | | $SiO_2$/(100)Si | Ref. 10 |
| Al | 80 | 20 | | $SiO_2$/(100)Si | Ref. 11 |
| Al | 2–5 | <70 | | Aluminum | Ref. 12 |
| Ti | ? | 200 | | Quartz | Ref. 9 |
| Ti | 4 | −100 | | (111)Si | Ref. 13 |
| Ti | 10 | 100 | | Glass | Ref. 14 |
| Au | 100 | 300 | | 7059 glass | Ref. 15 |
| Au | 3 | 50 | | Soda-lime glass | Ref. 16 |
| Au | 1 | 20 | | $MgF_2$/glass | Ref. 17 |
| Ni | 30 | 1200 | | (111)Si | Ref. 18 |
| Ni | 2–5 | 900 | | Nickel | Ref. 12 |
| Ni | 25 | 930 | | Nickel | Ref. 19 |
| Ge | 8 | 20 | | Fused silica | Ref. 20 |

ment hinges mostly on the accuracy of the elastic properties of the $SiO_2$ beams. Realistically, the assumed value of Young's modulus could be off by as much as $\pm 20\%$ with the resulting $\sigma_{total}$ values inaccurate by the same factor. This is not a serious problem, however, since 20% differences in film stress are often insignificant.

Table III also shows experimental values taken from the literature. These quoted values are all for evaporated films near 500 Å in thickness and were all measured on substrates of thickness greater than 100 $\mu$m. These large thicknesses usually necessitate the use of an interferometer technique for detecting the very small beam deflections during deposition. The substrate heating is considered negligible for the thick beams, so $\sigma_{total} \approx \sigma_{growth}$ for the referenced values.

The film stress for the Al, Au, and Ge films is found to be quite low and is consistent with the low values reported in the literature. This is also consistent with the observed behavior of these metal films as being free from any stress related cracks or peeling during deposition onto patterned photoresist. The Ni is found to be highly stressed in both this study and others.[15,19,20] Pt exhibits the highest average stress of the six metals studied. This is consistent with Pt's observed tendency to cause photoresist peeling for depositions in excess of 500 Å.

The only large discrepancy between these measured values and the reported values is in the case of Ti. The reasons for this disagreement could be many. Differences in the type and smoothness of substrates is likely to have a significant effect for very thin films of a highly reactive metal such as Ti. Other factors might include evaporation methods, evaporation rates, background pressures, and possible impurities in the Ti slugs. The Ti films used in this study are clearly in tension, but the Ti used in Ti/Al layered composites usually exhibits buckling tendencies that are characteristic of films in compression. Thus, it is quite possible that the stress in very thin Ti films is more sensitive to substrate conditions than the other five films.

## V. CONCLUSIONS

The micro-cantilever-beam technique has been shown to be very useful for determining stress in very thin films. Such thin films cannot be measured using standard wafer curvature techniques. Although the cantilever beams are very thin, they do not heat up appreciably during deposition because the $SiO_2$ is able to dissipate the heat radiatively. Thus, the thermal component of film stress is quite small. The results of this study are found to agree reasonably well with previously reported stress values in Al, Pt, Au, Ge, and Ni, but they do not agree in the case of Ti.

## ACKNOWLEDGMENT

The authors are grateful to Ed Korczynski from Watkins-Johnson Company in Scotts Valley for depositing the CVD $SiO_2$ films.

## REFERENCES

[1]P. M. Asbeck, C. P. Lee, and M. F. Chang, IEEE Trans. Electron Devices **ED-31**, 1377 (1984).
[2]S. Hong, T. P. Weihs, J. C. Bravman, and W. D. Nix, in *Thin Films: Stresses and Mechanical Properties,* edited by J. C. Bravman, W. D. Nix, D. M. Barnett, and D. A. Smith (Mater. Res. Soc. Symp. Proc. **130**, Pittsburgh, PA, 1989), p. 93.
[3]T. P. Weihs, S. Hong, J. C. Bravman, and W. D. Nix, in *Thin Films: Stresses and Mechanical Properties,* edited by J. C. Bravman, W. D. Nix, D. M. Barnett, and D. A. Smith (Mater. Res. Soc. Symp. Proc. **130**, Pittsburgh, PA, 1989), p. 87.
[4]*The CRC Handbook of Chemistry and Physics,* edited by R. C. Weast, 51st ed. (CRC Press, Cleveland, OH, 1970), p. D-55.
[5]*Thermophysical Properties of Matter,* edited by Y. S. Toulovkian (Plenum, New York, 1972), Vol. 5, *Specific Heat of Nonmetallic Solids,* p. 202.
[6]*Handbook of Heat Transfer Fundamentals,* edited by W. M. Rohsenow, J. P. Hartnett, and E. N. Ganic, 2nd ed. (McGraw-Hill, New York, 1985), pp. 14–21.
[7]*Thermophysical Properties of Matter,* edited by Y. S. Toulovkian (Plenum, New York, 1972), Vol. 9, *Thermal Radiative Properties of Coatings,* p. 1048.
[8]*Handbook of the Physicochemical Properties of the Elements,* edited by G.V. Samsonov (Plenum, New York, 1968).
[9]C. K. Hu, P. S. Ho, and D. Gupta, in *Thin Films: Stresses and Mechanical Properties,* edited by J. C. Bravman, W. D. Nix, D. M. Barnett, and D. A. Smith (Mater. Res. Soc. Symp. Proc. **130**, Pittsburgh, PA, 1989), p. 255.
[10]A. K. Sinha and T.T. Sheng, Thin Solid Films **48**, 117 (1978).
[11]M. Hershkovitz, I. A. Blech, and Y. Komen, Thin Solid Films **132**, 87 (1986).
[12]E. Klokholm, J. Vac. Sci. Technol. **6**, 138 (1969).
[13]J. Ann and S. J. Lewis, Thin Solid Films **23**, S67 (1974).
[14]H. C. Tong, C. M. Lo, and W. F. Traber, J. Vac. Sci. Technol. **13**, 99 (1976).
[15]S. S. Lau and R. C. Sun, Thin Solid Films **10**, 273 (1972).
[16]J. D. Wilcock, D. S. Campbell, and J. C. Anderson, Thin Solid Films **3**, 13 (1969).
[17]R. Abermann and R. Koch, Thin Solid Films **129**, 71 (1985).
[18]F. A. Doljack and R.W. Hoffman, Thin Solid Films **12**, 71 (1972).
[19]P. M. Alexander and R.W. Hoffman, J. Vac. Sci. Technol. **13**, 96 (1976).
[20]A. E. Ennos, Appl. Opt. **5**, 51 (1966).